P13R.7 RANGE EFFECTS ON REFLECTIVITY GRADIENTS IN TROPICAL BRAZIL

Roberto V. Calheiros* and Carlos Alberto A. Antonio

Meteorological Research Institute/IPMet - UNESP, Bauru, São Paulo, Brazil

1. INTRODUCTION

Presently, typical operations of NWP models use horizontal resolutions ranging from approximately 20 to 50 km in the global scale, and around 10 km for limited area in the mesoscale. Towards the end of this decade, plans call for a new generation of atmospheric models, substituting for those running today, which will be non-hydrostatic and will operate in the 1-3 km range of grid sizes (Caumont et al, 2005). For that, a significantly improved precipitation distribution representation should be achieved. As a matter of fact important programs approaching this issue have been carried out, e. g. the COST-717 European initiative, dedicated to promoting the use of radar data in both NWP and hydrological models. Yet, the modeling of hydrologic models which critically requires an accurate estimate of the spatial distribution of rainfall has driven an ever growing demand for high-resolution rainfall estimates based on radar. As a matter of fact, radar data resolutions for many hydrological applications involve unit cell sizes of less than (1x1) km^2. For operational settings where a limited number of radars are available for observations of areas at further ranges, yet demanding relatively better-resolved rainfall fields, the associated loss of definition of the radar derived rain structure is a matter of special concern. Such a situation is experienced in - and around - the State of S.Paulo, where a three-radar network surveys an space-extensive river basin network. This was a major factor prompting research and operations institutions in the State to develop efforts aiming to assess the magnitude of this (old) problem. In fact, Zawadzki back in 1982 presented a quite comprehensive paper were the precision of radar measurements are dealt with in a particularly appropriate way (Zawadzki, 1982). He points out the effects of the magnitude of gradients in a calculation of the mean rainfall over an area, and approaches the question of the change of the radar reflectivity factor and its spatial variability, with range. Following Zawadzki's work, Torlaschi and Humphries (1983) carried out a research on the statistics of reflectivity gradients, on the grounds of its relevance to improve the precision of radar measurements of the reflectivity patterns, from which the structure of precipitation is obtained. IPMet operates two radars of the S.Paulo network, and tackles the problem of retrieval of the structure of precipitation as a major topic of its research program. The most recent work on this at IPMet approached the representativeness of the rain field as observed by TRMM PR (Calheiros and Machado, 2005). The present paper is a preliminary verification of the distribution with range of reflectivity gradients from the Bauru radar (BRU) observations, centered on a summer season. Statistics are performed using operational products generated from BRU observations, which are available to the users, in an attempt to assess the extent to which they meet finer resolution requirements.

Cumulative probabilities that a given gradient is matched or exceeded were computed for different range rings, at along and cross-range directions, and for different periods within the rainy half of the year. Comparisons with other climatic areas is presented.

Indications stemming from the results, regarding a revision of operational products of the Bauru radar, are presented.

2. DATA AND PROCESSING

Data used are the original polar coordinate reflectivities from volume scans of BRU for the period of October, 2003 to March, 2004. Range rings for PPIs from successive elevations, i.e., 6.4 (ring 1), 2.7 (ring 2), 1.7 (ring 3), and 0.3 (rings 4 to 6) degrees, composing a CAPPI-like product at the average height of 3.5 km, contributed to the data set. Then reflectivities were classified within 6 range rings, i.e., from 15-45, 45-75, 75-105, 105-135, 135-165 and 165-195 km, respectively. For each range ring, reflectivity gradients were computed for both the along range and cross-range directions.

For the radial direction gradients, the absolute difference between a given bin and its forward neighbor were calculated along each ray. In the cross-range (circular) direction gradients were computed from the difference of a bin and its neighbor in the clockwise sense, for a constant range position around the radar. Results were then gathered in 30 classes of 1 dBZ. Cumulative Probabilities of a gradient being equal to or greater than a given value, i.e.,

$$\mathrm{P}\left(\frac{\Delta Z'}{\Delta r} \geq \frac{\Delta Z}{\Delta r}\right)$$

were generated.

Calculations were performed for each month, and curves were grouped in sets providing the following family of probabilities:

a) For all months in each ring,

b) For all rings in each month,

c) For all rings and the whole period from December to February

The curves in a) and b) were normalized to the gradient of 1 $dBZ.km^{-1}$. For the probability distributions in c) two sets were generated, one similar to a) and b), i.e., normalized to the gradient

* *Roberto V. Calheiros:* calheiros@ipmet.unesp.br

of 1 dBz.km^{-1}, and the other with the curves in rings 2 - to - 6 generated in reference of ring 1, i.e., considering the number of possible events as the number of gradients in the 0-1 dBZ interval in ring 1. For the probability distributions in c) two sets were generated, one similar to a) and b), i.e., normalized to the gradient of 1 dBz.km^{-1}, and the other with the curves in rings 2 - to - 6 generated in reference of ring 1, i.e., considering the number of possible events as the number of gradients in the 0 - 1 dBZ interval in ring 1.

3. RESULTS

Results are presented in the following set of graphs, i.e., Figures 1 to 6.

Figures 1 (a) to (f) are probability distributions for all rings, by month, along-range (radial) direction, while Figures 2 (a) to (f) are similar to Figure 1, but for cross-range (circular) direction. Figures 3 (a) to (f) present curves for all months, by ring, along-range (radial) direction. And Figures 4 (a) to (f) are similar curves, for cross-range (circular) direction.

Figures 5 (a) and (b) are curves for the December to February period, for each ring, and for radial and circular directions, respectively, with probabilities normalized to 1 dBZ km^{-1}. Figures 6 (a) and (b) are similar to 5 (a) and (b) but for probabilities in the rings normalized to curve for ring 1.

4. ANALYSIS

For the monthly evolution of curves for all rings, in the radial direction (Figures1), on the average the stratification increases from October to December, when in reaches a maximum, and then decreases towards February to March. In general, the curve for the first range ring is well separated of those for the other rings, which are near one another. From December to March curve for ring 2 shows a little more stratification.

For the circular direction (Figures 2), in general the same conditions apply, (except that the maximum occurs in November), but the stratification among the different rings is substantially more pronounced.

The curve for the different months, for the same ring (Figures 3), and for the radial direction, shows an oldest stratification for rings 1 and 2, and are all packed together for rings 3 to 6. For the circular direction (Figures 4), stratification is noticeably more pronounced than that for the radial direction, for all rings. Again, curves for rings 1 and 2 stratifies more than those for the outer rings.

In general, the three-month period December to February (Figures 5) shows, for the radial direction, a relatively moderate but clearly larger stratification than those for October, November and March (Figures 1). An approximately similar situation holds for the circular direction (Figures 5 and Figures 2). Figures 6 (a) and (b) shows the relative decrease of the number of gradients along the curve for each ring. For the lower gradient range, in the radial direction, gradients are about one order of magnitude less frequent for ring 6 as compared to ring 1. Situation is not much different for the circular direction.

For gradients greater than about 5 dBZ.km^{-1} comparisons are restricted to the inner rings. For rings 1 to 3 probabilities decrease by more than an order of magnitude. Again, differences among the directions are small.

Maximum gradients are around 23 - 24 dBZ.km^{-1} (with curves still statistically stable) for radial direction, and 25 - 26 dBZ.km^{-1} for circular direction. Considering the month of January, at peak summer, 10% of the gradients are bigger than about 10 - 11 dBZ.km^{-1} for ring 1, while for ring 6 the 10% threshold is only about 2 - 3 dBZ.km^{-1}. This holds for the radial curves. For the circular curves figures are 16 - 17 dBZ.km^{-1} and 3 - 4 dBZ.km^{-1}, respectively.

Also, while 50% of the gradients are bigger than about 3 - 4 dBZ.km^{-1} for ring 1 against ~ 1 dBZ.km^{-1} for ring 6, in the radial direction. For the circular direction figures are 4 - 5 dBZ.km^{-1} and 1 dBZ.km^{-1}, respectively.

5. COMMENTS AND CONCLUSIONS

The behavior of the curves indicates compatibility with the evolution of the rainy season. Three intervals are apparent, i. e., October in the dry-to-wet transition, December to February, for early & peak and March, for late summer up to mid-ranges for BRU (range rings 1&2), stratification is noticeable but for further ranges curves are mixed-up. With the broad antenna beam of BRU (~ 2^0) it is possible that beam filling effects vis-à-vis the dimensions of the cells prevent that range discrimination be manifested.

Because of the marked climate differences and antenna beamwidth (2^o for BRU and 1^o for Alberta) a comparison between gradient statistics for both regions may be particularly informative. The December to February curves for BRU show, on the average, a larger stratification for ring 1 when compared to similar Northern Hemisphere summer curves in the area of Alberta, Canada, for radial direction. For circular direction, however, differences are considerably smaller. A study on the combination of rain curves and antenna beamwidth for each area, should be explored in the search for evaluation of the range impacts on rain distribution representativeness of radar observations.

When results are preliminary compared with TRMM PR measurements for instance (Calheiros and Machado, 2005), it can be noticed that gradient statistics are compatible for both PR curves for the area covered by BRU, and the BRU curves for a range where PR resolutions is approximately matched (about 5km).

Results emphasize the importance of appropriately assess the range impact on BRU for rain structure reproducibility.

Figure 1 (a, b, c, d, e and f) – Cumulative probabilities for all rings for each month; radial direction.

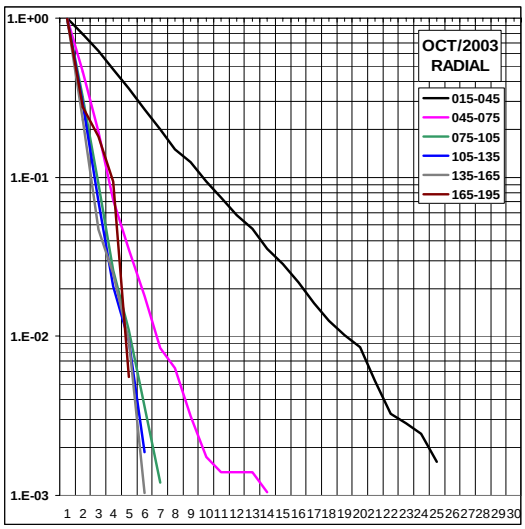

(1a)

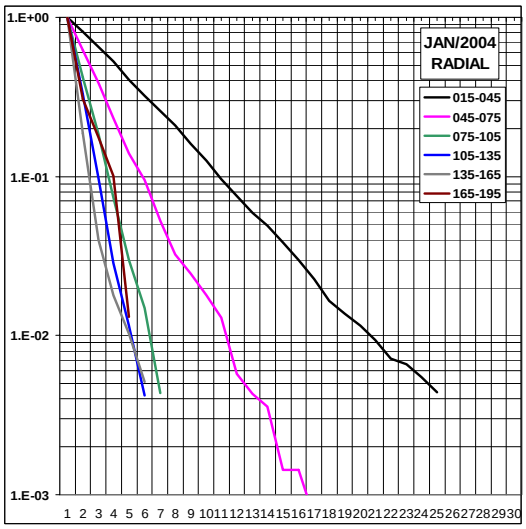

(1d)

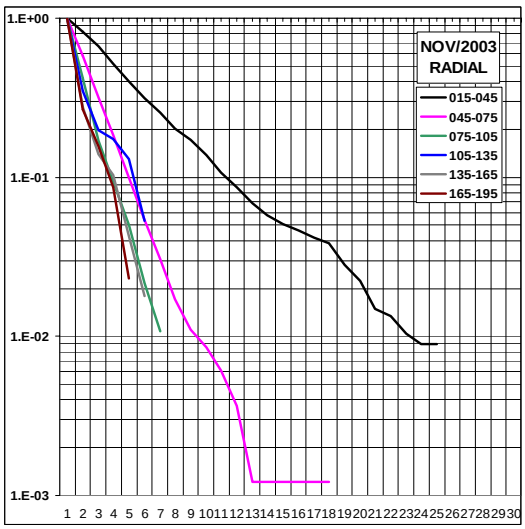

(1b)

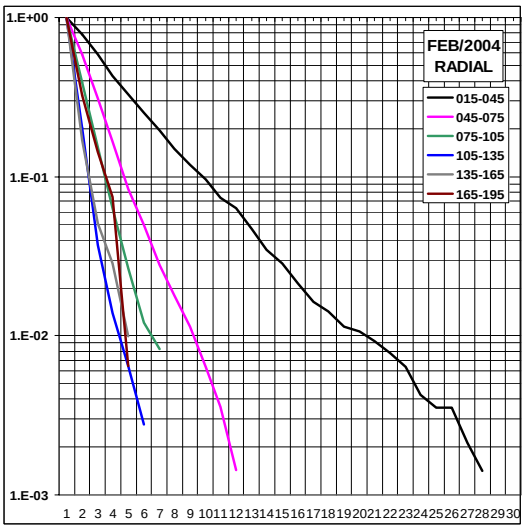

(1e)

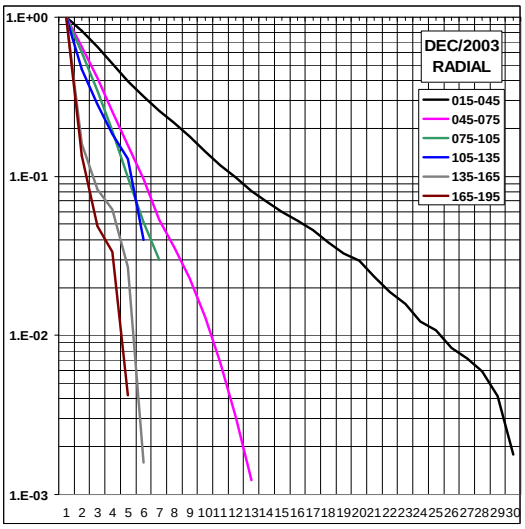

(1c)

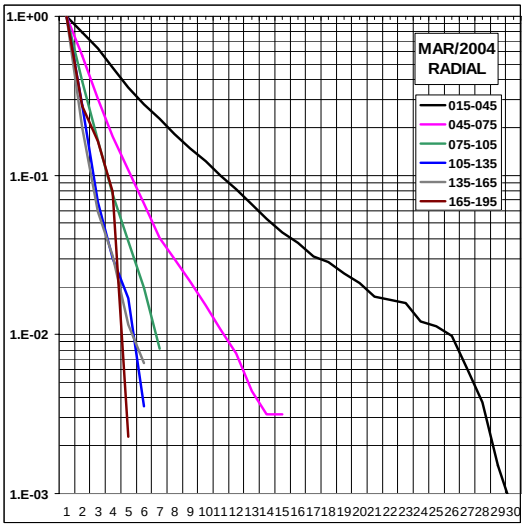

(1f)

Figure 2 (a, b, c, d, e and f) – Same as Figure 1, except that for circular direction.

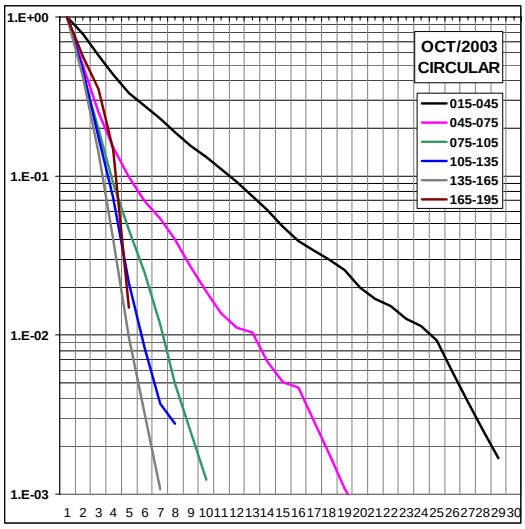

(2a)

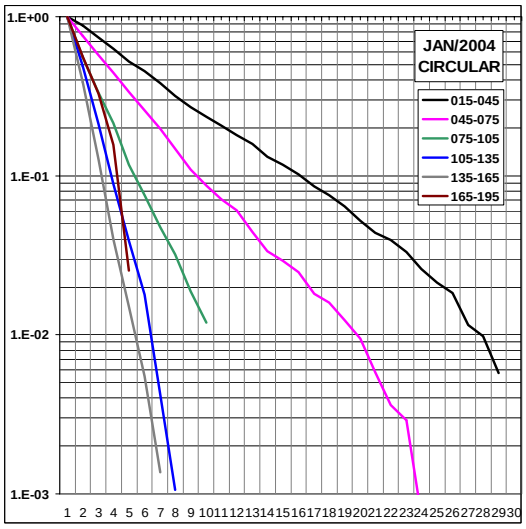

(2d)

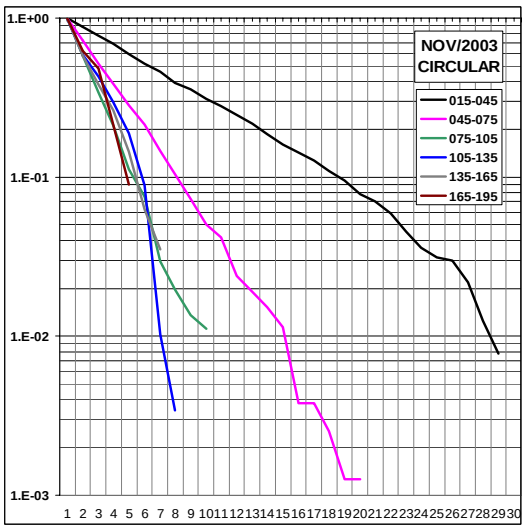

(2b)

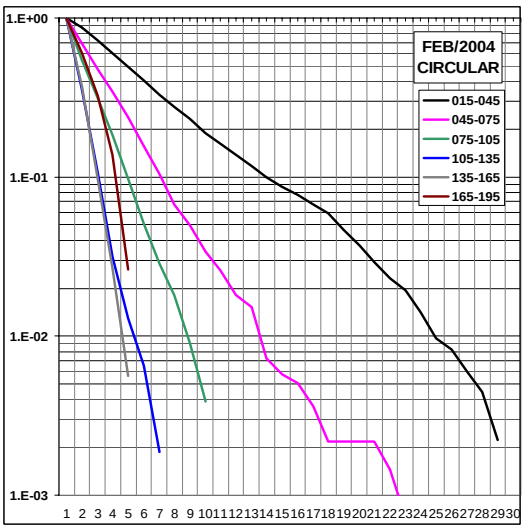

(2e)

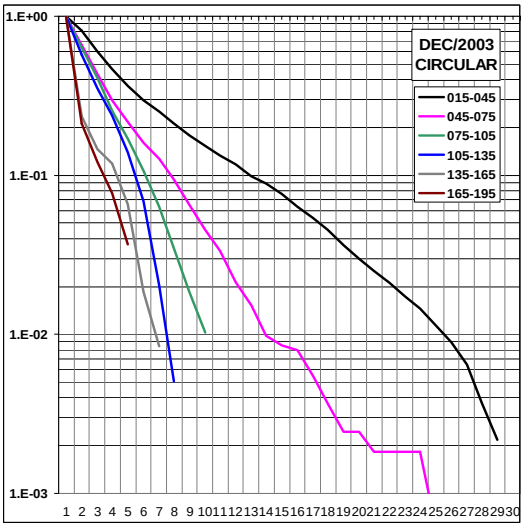

(2c)

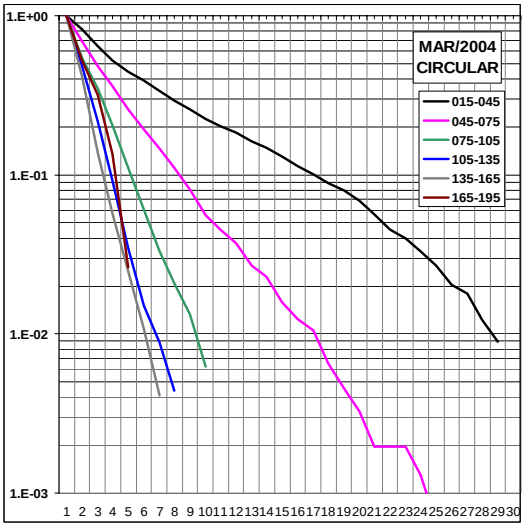

(2f)

Figure 3 (a, b, c, d, e and f) – Cumulative probabilities for all month for each range ring; radial direction.

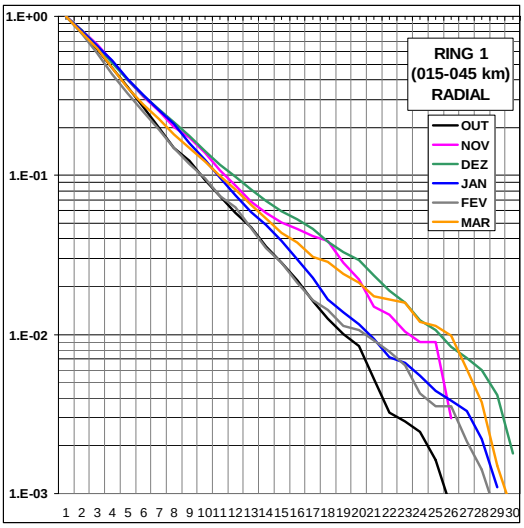

(3a)

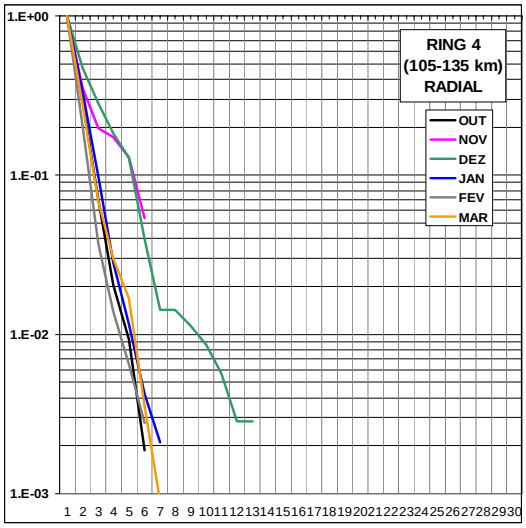

(3d)

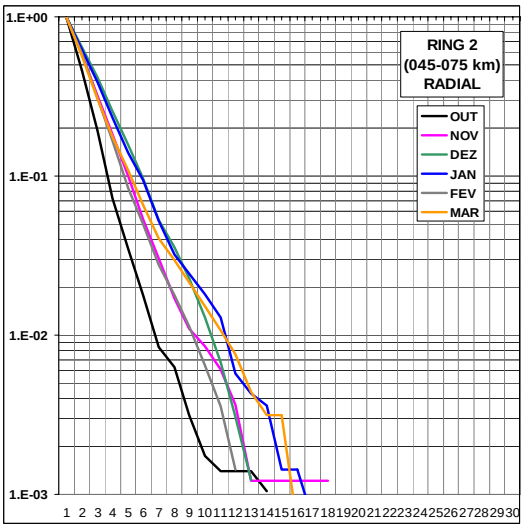

(3b)

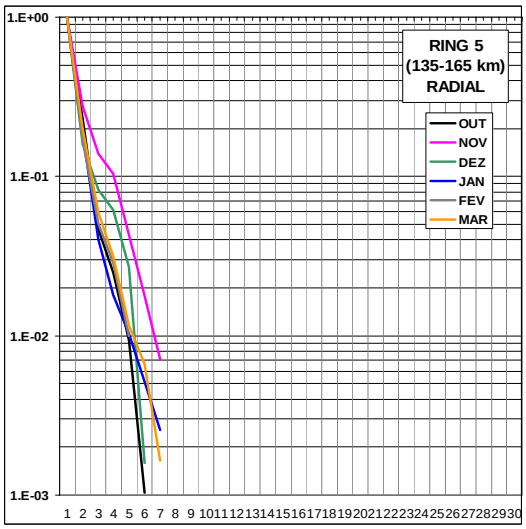

(3e)

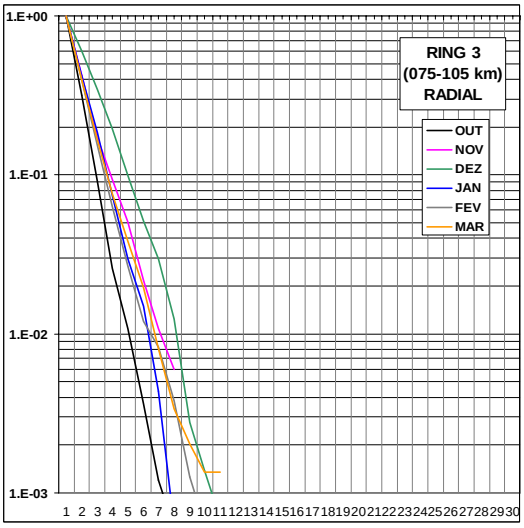

(3c)

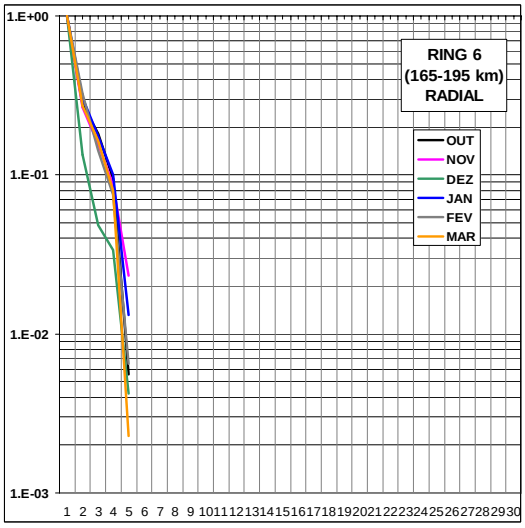

(3f)

Figure 4 (a, b, c, d, e and f) – Same as Figure 3, except that for circular direction.

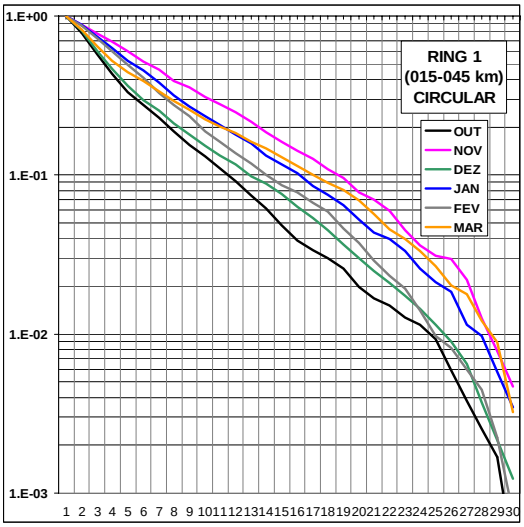

(4a)

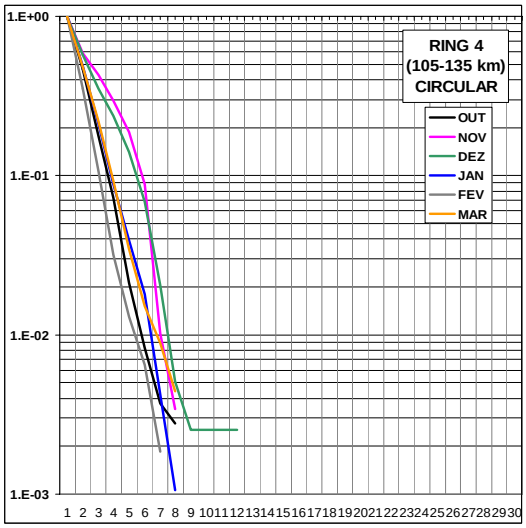

(4d)

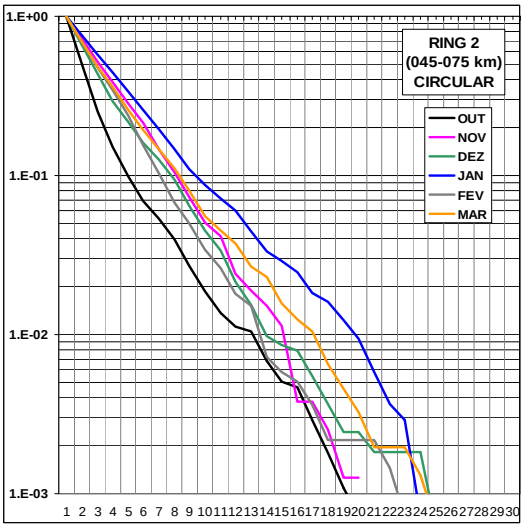

(4b)

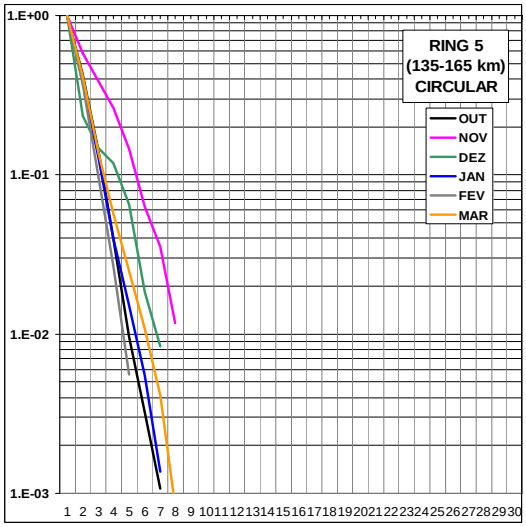

(4e)

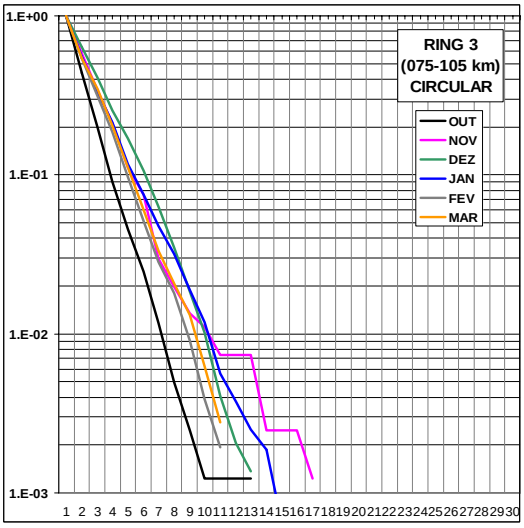

(4c)

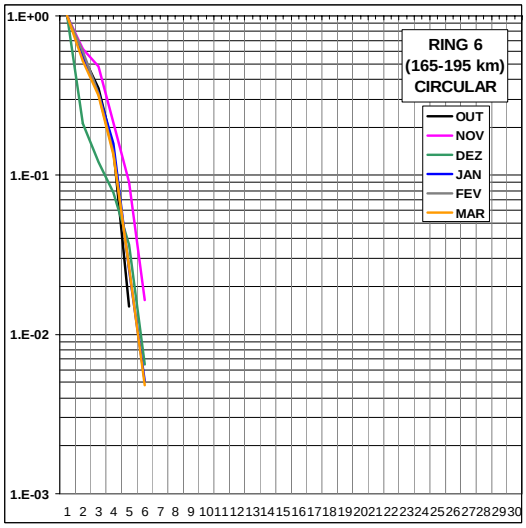

(4f)

Figure 5 (a and b) – Cumulative probabilities for the DEC-FEB period, for all rings; radial and circular direction.

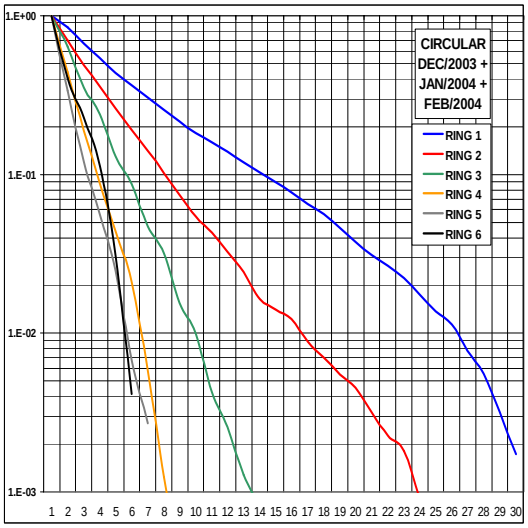

(5a)

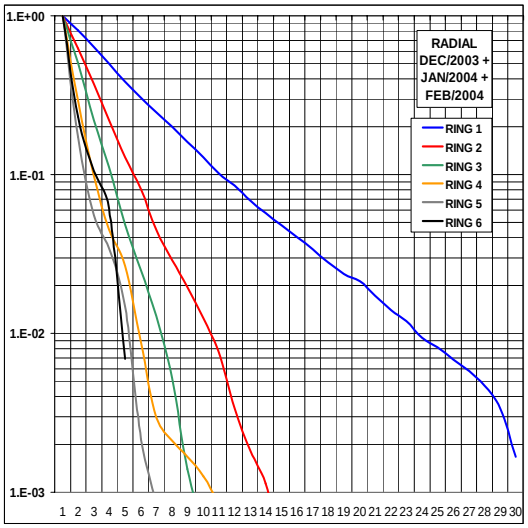

(5b)

Figure 6 (a and b) – Same as Figure 5 except that probabilities are refered to the number of gradients in first range ring for the 0 – 1 dBZ.km^{-1} class interval.

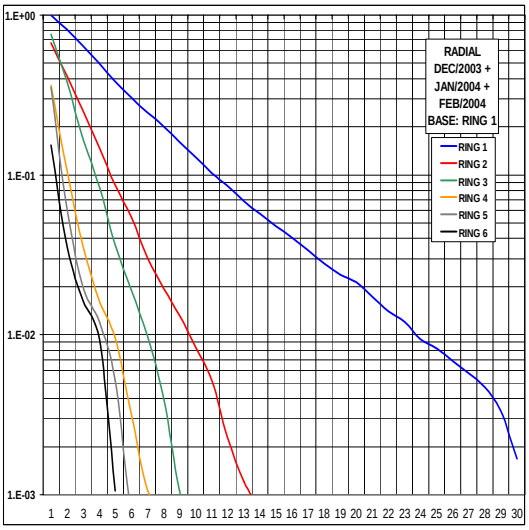

(6a)

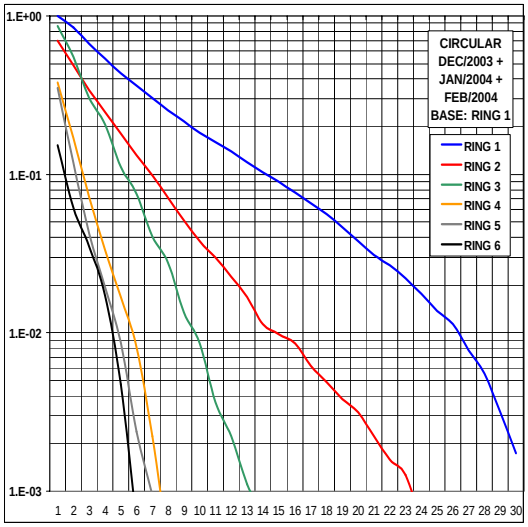

(6b)

6. REFERENCES

Calheiros, R.V., and R.Machado, "Rainfall representativeness at TRMM & GPM resolution", Proceedings of the 25th IEEE International Geoscience and Remote Sensing Symposium 2005 (CD-ROM), Seoul, Korea, 2005.

Caumont, O. and É.Wattrelot, V.Ducrocq, F.Bouttier, C.Guéguen, and G.L'Hénaff, " Towards a 1D+3Dvar Assimilation of Radar Reflectivities: Ongoing Results" CD-ROM 32nd Conference on Radar Meteorology, AMS, Albuquerque, NM, 2005.

I. Zawadzki, "Quantitative Interpretation of Weather Radar Measurements", Atmosphere-Ocean **20** (2) Canadian Meteorology and Oceanographic Society, 1982, p. 158-180.

Torlaschi, E. and R.G.Humphries, "Statistics of Reflectivity Gradients", 21st Conference on Radar Meteorology, AMS, Edmonton, Canada, 1983, p.173-175.